THE JOURNAL OF BIOLOGICAL CHEMISTRY
Vol. 279, No. 33, Issue of August 13, pp. 34514–34520, 2004
Printed in U.S.A.

Identification of Hyperreactive Cysteines within Ryanodine Receptor Type 1 by Mass Spectrometry*[S]

Received for publication, April 19, 2004, and in revised form, June 10, 2004
Published, JBC Papers in Press, June 14, 2004, DOI 10.1074/jbc.M404290200

Andrew A. Voss‡, Jozsef Lango§¶, Michael Ernst-Russell‡, Dexter Morin‡, and Isaac N. Pessah‡§‖

From the ‡School of Veterinary Medicine, Department of Molecular Biosciences, the §Center for Children's Environmental Health and Disease Prevention, and the ¶Department of Chemistry, University of California, Davis, California 95616

The skeletal-type ryanodine receptor (RyR1) undergoes covalent adduction by nitric oxide (NO), redox-induced shifts in cation regulation, and non-covalent interactions driven by the transmembrane redox potential that enable redox sensing. Tight redox regulation of RyR1 is thought to be primarily mediated through highly reactive (hyperreactive) cysteines. Of the 100 cysteines per subunit of RyR1, ~25–50 are reduced, with 6–8 considered hyperreactive. Thus far, only Cys-3635, which undergoes selective adduction by NO, has been identified. In this report, RyR1-enriched junctional sarcoplasmic reticulum is labeled with 7-diethylamino-3-(4′-maleimidylphenyl)-4-methylcoumarin (CPM, 1 pmol/μg of protein) in the presence of 10 mM Mg^{2+}, conditions previously shown to selectively label hyperreactive sulfhydryls and eliminate redox sensing. The CPM-adducted RyR1 is separated by gel electrophoresis and subjected to in-gel tryptic digestion. Isolation of CPM-adducted peptides is achieved by analytical and microbore high-performance liquid chromatography utilizing fluorescence and UV detection. Subsequent analysis using two direct and one tandem mass spectrometry methods results in peptide masses and sequence data that, compared with the known primary sequence of RyR1, enable unequivocal identification of CPM-adducted cysteines. This work is the first to directly identify seven hyperreactive cysteines: 1040, 1303, 2436, 2565, 2606, 2611, and 3635 of RyR1. In addition to Cys-3635, the nitrosylation site, six additional cysteines may contribute toward redox regulation of the RyR1 complex.

Redox modulation of proteins and ion channels through critical cysteines is thought to underlie the regulation of many intracellular signaling pathways. Initial studies of redox in biological systems focused on correlations of oxidative stress to the gross pathology of stroke (1, 2), atherosclerosis (3), and aging and neurodegeneration (4, 5). However, the study of redox has grown to include discrete and reversible regulation of cell physiology, often through high affinity signaling molecules such as H_2O_2 and NO (6). In biological systems, NO is broadly used for signaling by binding to specific cysteine sulfhydryls on target proteins. The high reactivity of NO toward protein sulfhydryls and heme groups may severely limit its free diffusion in biological systems, thus requiring a NO translocation and delivery system mediated by critical (reactive) protein sulfhydryls (7, 8). Examples of the many proteins NO is known to modulate include guanylate cyclase (9, 10), a Ca^{2+}-dependent potassium channel (11), *N*-methyl-D-aspartate receptors (12, 13), and ryanodine receptors (RyRs)[1] (14, 15).

The skeletal type RyR (RyR1) is a large (2.3-MDa) homotetrameric Ca^{2+} release channel of the sarcoplasmic reticulum that is subject to tight, multifaceted redox regulation, including oxidative activation and inhibition (16–19), subunit coordination (20), pO_2-dependent NO activation, possibly through reduced calmodulin inhibition (14), and transmembrane redox sensing capabilities (21–23). Additionally, Ca^{2+} release and single channel experiments suggest that oxidation, *S*-nitrosylation, and *S*-glutathionylation alter RyR1 sensitivity to Ca^{2+} and Mg^{2+} (24–26). All of these redox interactions are thought to be mediated by cysteines, of which there are 100 per monomer of RyR1. It is thought that ~25–50 of these cysteines are free and, based on reactivity, are commonly segregated into three to four classes (27–29). Of these, Cys-3635 has been shown to be selectively nitrosylated (15); whereas additional, yet unidentified cysteines are involved in redox regulation of the channel complex.

Biochemical evidence using the fluorogenic sulfhydryl probe 7-diethylamino-3-(4′-maleimidylphenyl)-4-methylcoumarin (CPM) to label junctional sarcoplasmic reticulum (JSR) preparations (0.1–1.0 pmol of CPM/μg of JSR protein) indicate, based on the labeling kinetics and pattern of proteins adducted, that RyR1 contains a group or class of hyperreactive sulfhydryls that are conformationally sensitive and exhibit the greatest reactivity in the closed state of the channel (30, 31). Additional biochemical and biophysical techniques indicate that this group of six to eight hyperreactive or critical cysteines bestow sensitivity to oxygen tension that is important in NO binding of Cys-3635 (14, 15, 29), determine RyR1 responsiveness to channel modulators (32), and confer the transmembrane redox sensing ability (21). The reversibility of RyR1 activation by redox potential changes and physiological levels of NO implies a delicate intracellular redox signaling mechanism. These functional data illustrate the critical role hyperreactive sulfhydryls play in redox regulation of RyR1; however, aside from the NO and calmodulin binding site of Cys-3635, the identity of

* This research was supported by National Institutes of Health (NIH) Grants 2RO1-AR43140 (to I. N. P.), 1PO1-ES11269 (to I. N. P.), and 2P42-ES04699 (to I. N. P. and J. L.) and NIH Training Grant ES07059 (to A. A. V.). The costs of publication of this article were defrayed in part by the payment of page charges. This article must therefore be hereby marked "*advertisement*" in accordance with 18 U.S.C. Section 1734 solely to indicate this fact.

[S] The online version of this article (available at http://www.jbc.org) contains additional text, Table S1, and Figs. S1–S10.

‖ To whom correspondence should be addressed. Tel.: 530-752-6696; Fax: 530-752-4698; E-mail: inpessah@ucdavis.edu.

[1] The abbreviations used are: RyR, ryanodine receptor; RyR1, skeletal-type ryanodine receptor; CPM, 7-diethylamino-3-(4′-maleimidylphenyl)-4-methylcoumarin; JSR, junctional sarcoplasmic reticulum; HPLC, high-pressure liquid chromatography; MS, mass spectrometry; MALDI, matrix-assisted laser desorption/ionization time-of-flight; ESI, electrospray ionization; MH, malignant hyperthermia; MHS, malignant hyperthermia susceptibility; CCD, central core disease; MOPS, 4-morpholinepropanesulfonic acid; TPCK, L-1-tosylamido-2-phenylethyl chloromethyl ketone.

the additional hyperreactive or critical cysteines remains uncertain.

This report identifies the hyperreactive sulfhydryls of RyR1 via post-translational modification with CPM and a mass spectrometric methodology. Labeling of JSR vesicles is performed with discriminating concentrations of CPM under conditions favoring RyR1 channel closure, which has been previously shown to specifically label hyperreactive cysteines within the channel complex and selectively eliminate its redox sensing capabilities (21, 30, 31, 33). Subsequent to this labeling reaction, the CPM-adducted RyR1 is subjected to tryptic digestion, sequential HPLC steps, and two methods of mass spectrometry. This methodology yields RyR1 sequence data and exact peptide masses corresponding to calculated CPM and hydrolyzed-CPM-adducted molecular masses, enabling the identification of 7 CPM-adducted cysteines of RyR1, including the NO binding site of Cys-3635. This work provides the first structural elucidation of most, and possibly all hyperreactive sulfhydryls of RyR1 that may regulate channel activity in response to changes in the local redox environment. A method is outlined that may have general applicability for identification of critical cysteines within redox-regulated proteins.

EXPERIMENTAL PROCEDURES

Materials—For sulfhydryl labeling, KCl and MOPS (>99.5%) were obtained from Sigma-Aldrich, $MgCl_2 \cdot 6H_2O$ from EM Scientific (Gibbstown, NJ), and CPM from Molecular Probes (Eugene, OR). JSR membrane preparation, CPM labeling, and electrophoresis were performed using NANOpure water from a Barnstead International purifier (model D4751, Dubuque, IA). Solvents for tryptic digestion and HPLC were High Purity Solvents from Burdick and Jackson (Muskegon, MI). Ammonium acetate (HPLC grade) and trifluoroacetic acid (protein sequence analysis grade) used in HPLC mobile phases were obtained from Fluka BioChemika (Bucks SG, Switzerland). Ultra Smooth Polypropylene or Low Retention Microcentrifuge Tubes (0.65 or 1.5 ml, Island Scientific, Bainbridge Island, WA) were used during tryptic digestion and manual collection of HPLC fractions. Concentrations during in-gel digestion and of HPLC fractions were performed using an SVC-200H Savant SpeedVac concentrator system (GMI, Inc., Albertville, MN). Electrophoresis gels were cast with 30% Duracryl (Genomic Solutions, Ann Arbor, MI). Protein assays were based on the method described in Lowry *et al.* (34).

Membrane Preparation—JSR was isolated from male New Zealand White rabbit fast-twitch skeletal muscle using the method previously described in Saito *et al.* (35).

CPM Labeling of JSR—CPM was prepared and used as described in Liu *et al.* (30). The labeling of the most reactive cysteines present in JSR was performed as previously described, with solutions degassed under vacuum. JSR vesicles were incubated while continuously stirring in RyR closed buffer (100 mM KCl, 20 mM MOPS, and 10 mM $MgCl_2$, pH 7.4) and 1 μg/ml leupeptin from Sigma-Aldrich at 37 °C for 3–5 min prior to addition of CPM (1 pmol/μg of JSR protein) to a final volume of 25 ml. The reaction proceeded for 1 min before being placed on ice, a time previously shown under closed conditions to complete the reaction (30). CPM-labeled JSR was pelleted at 146,000 × *g* ($r_{average}$) and 4 °C for 3 h using a Ti-50.2 rotor (Beckman) and resuspended in RyR closed buffer.

Gel Electrophoresis—Ensuing protein denaturation in Laemmli Sample Buffer from Bio-Rad Laboratories (Hercules, CA) at 37 °C for 1 h, CPM-RyR1 was isolated from labeled JSR vesicles using SDS-PAGE in large format gels (20 × 20 × 0.1 cm) under constant 25 mA. The resolving gel (pH 8.8) consisted of a two-phase composition, the bottom 60% consisting of 10% acrylamide and the top 40% consisting of 3–10%; a 10-well 3% stacking gel (pH 6.8) was also used.

CPM-RyR Digestion—In-gel tryptic digestion procedures were based on methods described in Shevchenko *et al.* (36) and Wilm *et al.* (37). CPM-labeled RyR1 excised from each SDS-PAGE gel was washed thoroughly four times (15 min each) with water, diced into approximately 1-mm squares, and dried via the SpeedVac in 1.5-ml microcentrifuge tubes (3–6 tubes). Gel pieces were subsequently reduced with 10 mM dithiothreitol in 100 mM NH_4HCO_3 (pH 8, 55 °C) for 1 h and alkylated with 55 mM iodoacetamide in 100 mM NH_4HCO_3 for 45 min in the dark at room temperature. Gel pieces were washed with 100 mM NH_4HCO_3 and partially dehydrated with acetonitrile before complete dehydration via SpeedVac. Finally, the CPM-RyR1 was digested in 50% NH_4HCO_3, pH 7.8–8.0, containing sequence grade TPCK-modified trypsin (catalog no. V5111, Promega, Madison, WI) at a final concentration range of 10 to 25 ng/μl (37 °C) for 24 h. Peptides were extracted once each with 0.1% trifluoroacetic acid and then 5% formic acid-acetonitrile (50:50). The digested CPM-RyR1 from each gel was then combined and concentrated by SpeedVac to 100 μl for analytical HPLC analysis.

Sequential HPLC—Initial separation of tryptic digested CPM-labeled RyR was performed using a Vydac (catalog no. 218TP52, Hesperia, CA) analytical C-18 reverse phase HPLC column (2.1-mm inner diameter × 25-cm length) on a Waters 600 system (Milford, MA). Separations were performed at 0.5 ml/min using mobile phases A (25 mM ammonium acetate in 10% acetonitrile) and B (22.5 mM ammonium acetate in 80% acetonitrile) with initial conditions of 83% A and 17% B that changed linearly to 70% A and 30% B over 80 min, then to 100% B over 10 min. Separation was completed with 100% B for 10 min. The eluant was monitored with a variable wavelength Hewlett-Packard (Palo Alto, CA) 1100 UV detector monitoring absorbance at UV 214 nm for peptide detection and a Shimadzu (Kyoto, Japan) 535 fluorescence detector with a standard flow cell (12 μl) monitoring emission at 469 nm from excitation at 384 nm for detection of CPM-adducted peptides.

Fluorescence fractions from analytical HPLC were subjected to additional separation using a Vydac (catalog no. 218TP51) microbore C-18 reverse phase HPLC column (1.0-mm inner diameter × 25-cm length) with an ABI model 140B Solvent Delivery System. Separations were performed at 80 μl/min using mobile phase A (0.1% trifluoroacetic acid) and B (0.085% trifluoroacetic acid in 70% acetonitrile) with an initial condition of 95% A that decreased linearly to 65% over 10 min, then to 40% over 50 min, and then to 5% over 10 min. Separation was completed with 5% A for 5 min. Samples were loaded in multiple injections under the initial conditions, and the signal was allowed to return to baseline before onset of the run. A dual detection system was again employed, using an ABI model 785A Programmable Absorbance Detector monitoring absorbance at UV 214 nm for peptide detection and a Shimadzu (Kyoto, Japan) 535 fluorescence detector with a 2-μl semi-micro flow cell (catalog no. 20662817) monitoring emission at 469 nm from excitation at 384 nm for detection of CPM-adducted peptides.

Mass Spectrometry—Samples were analyzed in a matrix-assisted laser desorption/ionization time-of-flight (MALDI-TOF) mass spectrometer (Biflex III, Bruker Daltonics, Bremen, Germany) and in a quadrupole orthogonal time-of-flight mass spectrometer with *QqT* geometry, where *Q* is the quadrupole analyzer, *q* is the R_F-only quadrupole, and *T* is the time-of-flight analyzer (QSTAR, Applied Biosystems, Foster City, CA) for direct electrospray MS (ESI) and tandem ESI (ESI MS/MS) experiments. In both cases the spectra were generated in positive ion mode.

The MALDI-TOF instrument was equipped with a nitrogen laser operating at an output of 337.1 nm with a pulse width of 3 ns and a repetition rate of 6 Hz. The instrument was operated in reflector mode, 19.3-kV acceleration potential, 20.0-kV reflector potential, 2- to 4-ns time base, and 10- to 30-ms delay. The output signal of the detector was digitized at a sampling rate of 500 MHz/channel using a 1-GHz Lecroy digitizer. A camera mounted on a microscope allowed inspection of the sample crystallization. The crystals on the target were sampled randomly, with major coverage of the spot. External calibration was performed with angiotensin II (Sigma, A9525) and somatostatin 28 (Sigma, S6135) with molecular masses according to the $(M+H)^+$ ions at *m/z* 1046.53 Da (angiotensin II, monoisotopic mass), *m/z* 3147.47 Da (somatostatin 28, monoisotopic mass). For analysis, first a 0.5-μl matrix solution, α-cyano-4-hydroxycinnamic acid (Hewlett Packard, part number G2054-85010) then 0.5 μl of the sample (protein digest) were spotted onto the stainless steel tip and allowed to dry at room temperature.

The quadrupole orthogonal time-of-flight mass spectrometer was controlled by Analyst-QS version 1.0 software with Service Pack 3 installed. This instrument was equipped with a nano-spray ionization source (Protana, Odense, Denmark). Voltage on the Protana "medium" capillary tips was 900 V. External two-point calibration was performed using the singly charged ions of CsI and a peptide with nominal mass of 828.5 Da. Mass accuracy was typically better than 10 ppm, and resolution was typically better than 7000 full-width half-maximum. The flow rate of the nanospray source was ~25–50 nl/min. Nitrogen was employed as the curtain gas at 25 arbitrary units. The orifice voltage was set at 80 V for all samples, whereas the focusing ring was set to 250 V and the skimmer was kept at 30 V. The TOF analyzer was set to acquire spectra at a rate of 7 kHz over the mass range 100–3000 Da. The resultant spectra are the averages of 100–300 consecutive spectra.

MS Data Analysis—The generated mass spectral data were transformed into ASCI format for analysis using MassLynx 4.0 software,

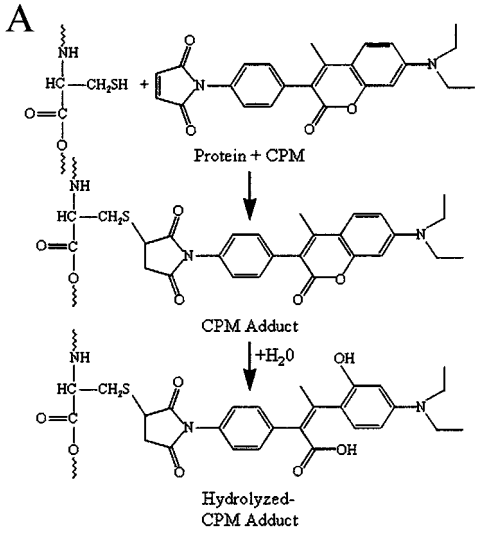

FIG. 1. **Chemistry of CPM adduct formation and procedural outline for identification of CPM adducts.** *A*, chemical reaction illustrating CPM forming a Michael adduct with a protein sulfhydryl and undergoing a subsequent hydrolysis of the chromen ring. *B*, a schematic outlining the mass spectrometric methodology to identify CPM-adducted sulfhydryls of RyR1.

including the MaxEnt module for signal reconstruction (Waters/Micromass, Manchester, UK). Theoretical masses for 0, 1, 2, and 3 positively charged peptides from full tryptic digestion of RyR1 were generated using the MassLynx 4.0 protein peptide editor module. Additional peptide masses were calculated for all cysteine containing peptides based on adduction by the 402.16-Da CPM and 420.17-Da hydrolyzed-CPM (see Fig. 1*A*). For peptides containing two cysteine residues, CPM modifications are assumed identical. Additionally, peptides with one uncleaved Arg or Lys were allowed (first order incompletion). The mass calculations for unmodified RyR1 peptides containing cysteines and all modified RyR1 peptides were merged into one Microsoft Excel data base used to screen masses generated by MS. Peptide sequence information obtained from MS/MS experiments facilitates the data base mass comparisons and was used whenever possible. A detailed description of the data base generation and the data base, are given in the Supplemental Material.

RESULTS

CPM Labeling, SDS-PAGE, and In-gel Tryptic Digestion—A schematic illustrating the identification procedure is included in Fig. 1*B*. The paramount first step in the identification of RyR1 hyperreactive sulfhydryls is their specific labeling by CPM under physiologically relevant, well characterized conditions. To achieve this, RyR1 hyperreactive sulfhydryls were labeled as described under "Experimental Procedures" using discriminating amounts of CPM to label JSR (1 pmol of CPM/μg of protein), a membrane fraction containing proteins, and cellular components necessary for normal RyR1 function. The CPM labeling of JSR was performed 24 times over a period of 2 days, yielding ~15 mg of CPM-labeled JSR protein. At 1 pmol of CPM/μg of protein, the JSR used in this procedure produced CPM labeling rate constants under RyR1 open (20 μM Ca^{2+}) and closed (10 mM Mg^{2+}) of 0.00156 ± 0.00003 and 0.04469 ± 0.00016 s^{-1}, respectively. The significantly faster rate of thioether adduct formation under channel-closed conditions was consistent with previously reported results (30, 31). Additionally, CPM labeling of JSR under the RyR1 closed conditions used in this procedure has been previously shown to selectively eliminate RyR1 redox sensing (21) through specific binding of hyperreactive sulfhydryls (30, 31, 33).

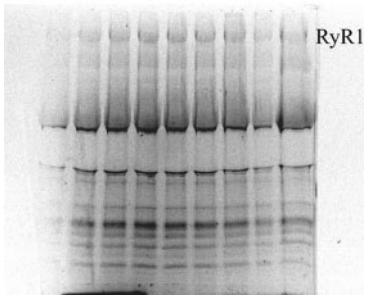

FIG. 2. **Fluorescent profile of SDS-PAGE.** A fluorescence image of a representative SDS-PAGE separation of CPM-labeled JSR, with CPM-labeled RyR1 representing the lowest mobility band that was subsequently excised for in-gel tryptic digestion.

Size separation of CPM-RyR1 thioether adducts from the other JSR proteins was achieved using SDS-PAGE (a total of nine gels). A representative gel image illustrating the CPM fluorescence pattern is shown in Fig. 2, which is consistent with previously reported results (30, 31). The additional fluorescent bands are currently under a similar investigation. In addition to providing clean separation of the CPM-RyR1 adducts, SDS-PAGE provides an excellent medium for full tryptic digestion, which generally yields doubly charged cationic peptides that are highly amenable to MS sequencing. Digested peptides were extracted from the gel matrix, frozen with liquid N_2, and stored at −80 °C until separated by analytical HPLC. Successful tryptic digestion was verified in subsequent HPLC profiles.

HPLC Separations—A monomer of RyR1 (5037 amino acids) generates 505 predicted tryptic cleavage products that can be separated using sequential steps of analytical and microbore HPLC. For each large format gel (nine total), the digested RyR1 peptides were subjected to C-18 reverse phase analytical HPLC. Fluorescence detection of CPM-adducted peptides using 384-nm excitation and 469-nm emission wavelengths generated a similar pattern for all nine analytical HPLC separations; a representative chromatogram is included in Fig. 3*A*. Each analytical HPLC chromatogram contained seven to eight dominant fluorescence peaks that were combined and concentrated into groups A, B, and C based on retention times: group A containing two to three peaks and eluting from 23 to 31 min, group B containing one peak eluting from 31 to 38 min, and group C containing three to four peaks eluting from 49 to 64 min (Fig. 3*A*). Several smaller fluorescence peaks were routinely observed between groups B and C (44–48 min), which were not analyzed due to their relatively low intensity and variable profile. Of the total fluorescence signal, groups A, B, and C represent 60–70%, with the variable peaks between groups B and C contributing ~10%. Minor peaks and a slightly increasing baseline constitute the remaining fluorescence signal.

To achieve greater resolution of the CPM-adducted RyR1 peptides, a microbore HPLC separation was performed on the pooled and concentrated analytical HPLC groups, monitoring fluorescence and UV absorbance. A representative chromatogram of group C in Fig. 3*B* illustrates improved, but incomplete resolution of the fluorescence peaks. Complete resolution of individual CPM-adducted RyR1 peptides occurred in subsequent MS analysis. One microbore separation was performed

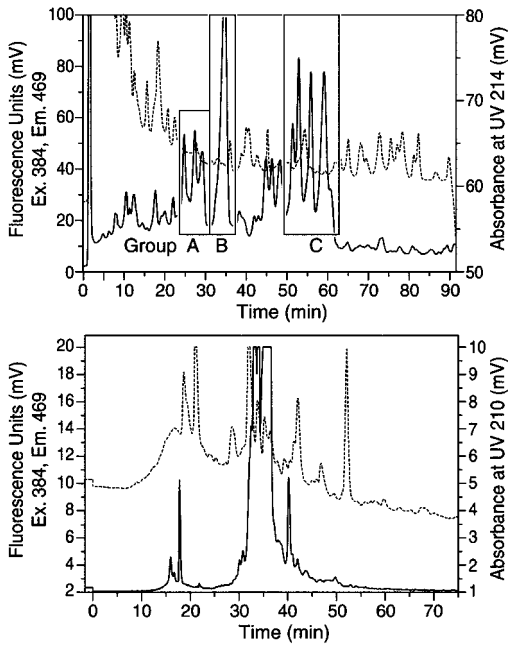

FIG. 3. **Sequential reverse phase HPLC separation of CPM-adducted RyR1 tryptic peptides.** Representative analytical (*A*) and microbore (*B*) HPLC chromatograms illustrating the fluorescence due to CPM (*solid line*) and absorbance at 214 nm for analytical and 210 nm for microbore (*dashed line*) HPLC.

on Group B, whereas two were performed on groups A and C. The second group C chromatogram is included in Fig. 3*B*. To possibly facilitate MS ionization, each fluorescent microbore fraction was partially hydrolyzed in 1% formic acid for 1 week under the storage conditions of 4 °C. Prior to MS analysis, samples were concentrated via SpeedVac to ~10 μl, and acetonitrile was added to improve spray ionization efficiency.

Mass Spectrometry—To identify the specific cysteines adducted by CPM, the fluorescence eluant from microbore HPLC was subjected to MS analysis using two methods, direct MALDI-TOF MS (MALDI) and ESI MS/MS (ESI). Both provide accurate peptide mass determinations with mass accuracies of 50 ppm for MALDI and better than 10 ppm for ESI. The ESI was the primary choice due to the higher mass accuracy and sequencing capabilities. Analysis of all fluorescent microbore eluants required 12 MALDI, 11 direct ESI, and 67 ESI product ion MS experiments. The charge state of the ions measured by MS are denoted by $(M+nH)^{n+}$, where n is the charge of the ion due to the addition of protons. In total, 7 CPM-adducted cysteines were identified from 6 digested peptides (one containing two cysteines), summarized in Table I and outlined as follows: 1) Cys-3635 (peptide 3631–3637) adducted by hydrolyzed-CPM was found in three microbore HPLC fractions of group C based on the theoretical peptide mass of $(M+H)^+$ 1185.58 Da and MS/MS sequence identification. The peptide fragment was found in MALDI as a high intensity signal at $(M+H)^+$ 1185.71 Da (Fig. 4*A*) and in direct ESI by a low intensity signal at $(M+2H)^{2+}$ 593.24 Da that corresponds to the predicted value of $(M+H)^+$ 1185.58 Da (Fig. 4*B*). This ion was selected for ESI MS/MS analysis and produced a fragmentation pattern indicating CPM adduction of peptide 3631–3637 (Fig. 4*C*). 2) Cys-1303 (peptide 1303–1324) adducted by CPM and hydrolyzed-CPM was found in microbore HPLC fractions of group C (two fractions) and B (one fraction), respectively. Identification was based on the theoretical peptide masses of $(M+H)^+$ 2564.21 Da (CPM adduct) and $(M+H)^+$ 2582.22 Da (hydrolyzed-CPM adduct) and achieved through MALDI, ESI, and ESI MS/MS. For the group B fraction, Fig. 4*D* illustrates the MALDI spectrum with a low intensity signal at $(M+H)^+$ 2582.26 Da. In Fig. 4*E*, the direct ESI spectrum contains low intensity signals at $(M+3H)^{3+}$ 861.44 Da and $(M+4H)^{4+}$ 646.32 Da that correspond to the predicted value of $(M+H)^+$ 2582.22 Da. The ESI MS/MS spectrum of the $(M+3H)^{3+}$ 861.44-Da peptide yields a fragmentation pattern that indicates peptide 1303–1324 adducted by hydrolyzed-CPM (Fig. 4*F*). For microbore HPLC group C, the MALDI spectra do not contain useful information about this peptide due to low ionization efficiency and/or concentration. However, a direct ESI experiment produces a strong signal at $(M+3H)^{3+}$ 855.40 Da that corresponds to the predicted value of $(M+H)^+$ 2564.21 Da for CPM-adducted peptide 1303–1324 (Supplemental Fig. 1). ESI MS/MS analysis of this triply charged ion produced a fragmentation pattern further indicating CPM adduction of Cys-1303 in the 1303–1324 peptide (Supplemental Fig. 2). 3) Cys-2565 (peptide 2565–2575) adducted by CPM was detected in one microbore HPLC fraction of group C based on the theoretical peptide mass of $(M+H)^+$ 1603.74 Da and MS/MS sequence identification. The MALDI spectrum in Fig. 4*A* illustrates a high intensity signal corresponding to $(M+H)^+$ 1604.09 Da. In Fig 4*B*, direct ESI reveals strong signals at $(M+2H)^{2+}$ 802.40 Da and $(M+3H)^{3+}$ 534.91 Da, respectively. ESI MS/MS analysis of the $(M+3H)^{3+}$ 534.91 Da peptide illustrates a fragmentation pattern that matches the theoretical decomposition for peptide 2565–2575 (Supplemental Fig. 3). 4) Cys-2606 and Cys-2611 (peptide 2598–2612) with both cysteines adducted by hydrolyzed-CPM was detected in one microbore HPLC fractions of group A based on the theoretical peptide mass of $(M+H)^+$ 2576.17 Da. The fraction yielded a MALDI spectrum with a low intensity peak at $(M+H)^+$ 2576.30 Da, corresponding to the predicted $(M+H)^+$ 2576.17 Da for hydrolyzed-CPM adduction of Cys-2606 and Cys-2611 (Supplemental Fig. 4). A direct ESI spectrum transformed to show the single charge state and reduce the noise illustrates an intense signal at $(M+H)^+$ 2576.21 Da, corresponding to the predicted $(M+H)^+$ 2576.17 Da (Supplemental Fig. 5). 5) Cys-1040 (peptide 1037–1044) adducted by hydrolyzed-CPM was detected in two microbore HPLC fractions of group A based on the theoretical peptide mass of $(M+H)^+$ 1311.60 Da. Each fraction yielded a separate MALDI spectrum, one indicating a strong signal at $(M+H)^+$ 1311.47 Da (Supplemental Fig. 6) and the other a strong signal at $(M+H)^+$ 1311.60 Da (Supplemental Fig. 7). 6) Cys-2436 (peptide 2436–2447) adducted by CPM was detected in one microbore HPLC fraction of group B based on the theoretical peptide mass of $(M+H)^+$ 1699.80 Da. A direct ESI spectrum transformed to the single charge state illustrates a strong signal at $(M+H)^+$ 1699.99 Da (Supplemental Fig. 8).

These cysteines represent high probability matches to theoretical predictions of CPM- or hydrolyzed-CPM-adducted peptides of RyR1. To further ensure proper identification, the obtained masses are also screened against theoretical digests of unlabeled RyR1 and the TPCK-modified porcine trypsin (Swiss-Prot P00761, with lysines methylated) used for digestion. The peptide masses obtained do not match any of these theoretical digests masses. Cysteines identified with the highest probability are 1303, 2565, and 3635, which are detected by MALDI, direct ESI, and ESI MS/MS. Cysteines 2606 and 2611 also represent high probability matches being identified by both MALDI and direct ESI. Although still with high probability, cysteines 1040 and 2436 are identified by MALDI and direct ESI, respectively.

Two additional cysteines were also tentatively identified. Direct ESI transformed to the single charge state detected what appears to be two overlapping signals yielding a mass $(M+H)^+$ of 2139.29 Da (Supplemental Fig. 9), closely matching

TABLE I

Summary of MS results, listing the seven redox-sensing cysteines identified

Listed are the cysteines identified by amino acid number, the corresponding RyR1 peptide sequence with the modified cysteines in bold and underlined (**C**), whether the cysteine modification was by CPM or hydrolyzed CPM (Hyd-CPM), the analytical HPLC group containing the CPM-adducted peptide (A, B, or C) and the MS methodology detecting the CPM-adducted peptide, including direct MALDI-TOF (MALDI), direct ESI (ESI), and tandem ESI (MS/MS). For direct MALDI and ESI, the theoretical (in parentheses) and obtained ion masses (Da) are listed next to the analytical HPLC group. The multiple listing for most cysteines indicate the corresponding peptide was detected in multiple microbore HPLC fractions, each one listed.

Cys position	RyR1 segment	Modification	Analytical HPLC group, $(M+H)^+$ found (theoretical)		
			MALDI	ESI	MS/MS
			Da		
1040	DSL**C**QAVR	Hyd-CPM	A, 1311.61 (1311.60)		
		Hyd-CPM	A, 1311.47 (1311.60)		
1303	**C**TAGATPLAPPGLQPPAEDEAR	Hyd-CPM	B, 2582.21 (2582.22)	B, 2582.22 (2582.22)	B
		CPM		C, 2564.21 (2564.21)	C
		CPM		C, 2564.14 (2564.21)	
		CPM		C, 2564.20 (2564.21)	
2436	**C**APEMHLIQAGK	CPM		B, 1699.99 (1699.80)	
2565	**C**APLFAGTEHR	CPM	C, 1604.09 (1603.74)	C, 1603.82 (1603.74)	C
2606 and 2611	AQRDVIED**C**LMAL**C**R	Hyd-CPM	A, 2576.30 (2576.17)	A, 2576.21 (2576.17)	
3635	AVVA**C**FR	Hyd-CPM	C, 1185.71 (1185.58)	C, 1185.66 (1185.58)	C
		Hyd-CPM	C, 1185.73 (1185.58)	C, 1185.58 (1185.58)	
		Hyd-CPM	C, 1185.91 (1185.58)		

the predicted peptide mass of $(M+H)^+$ 2138.96 Da for CPM adducted Cys-120 in peptide 116–130. Similarly, ESI also detected another set of overlapping signals indicating a mass of $(M+H)^+$ 2334.46 Da (Supplemental Fig. 10), possibly corresponding to the predicted mass of $(M+H)^+$ 2335.19 Da for CPM-adducted Cys-3193 in peptide 3180–3196. These obtained masses do not match theoretical peptide masses from tryptic digestion of unmodified RyR1 or self-digestion of TPCK modified trypsin. However, these cysteines are presented with a caveat due to mass ambiguity and that neither MALDI nor ESI MS/MS analysis supported the identifications.

DISCUSSION

Several lines of biochemical and biophysical evidence indicate the central role 6–8 critical or hyperreactive sulfhydryls of RyR1 play in conferring channel sensitivity to modulators and in sensing O_2 tension and transmembrane redox potentials (14, 21, 25, 26). Identification of Cys-3635 as the only sulfhydryl adducted by NO under physiological conditions is heretofore the only structural information regarding the hyperreactive sulfhydryls of RyR1 (15). The scarcity of structural information likely results from difficulties in isolating and digesting the large (~2.3 MDa tetramer), membrane-bound RyR1, which contains 100 cysteines per monomer. In addition, specific labeling of hyperreactive sulfhydryls requires fully functional RyR1, conditions that include discriminating, undisruptive concentrations of labeling reagent and a membrane fraction containing the numerous RyR1 accessory proteins. This work uncovers the primary sequence location of seven hyperreactive sulfhydryls that may be involved in conferring redox-sensing properties to the RyR1 channel complex and describes the mass spectrometric methodology based on post-translational modification employed in the identification.

Initial challenges in identifying the hyperreactive sulfhydryls include labeling RyR1 in a physiologically relevant environment containing the necessary accessory proteins and subsequently isolating the CPM-RyR1 from this milieu. Adherence to conditions previously described in the initial detection of hyperreactive sulfhydryls (30, 31) and the characterization of the transmembrane redox sensor (21) ensure the specific CPM labeling of redox-sensitive sulfhydryls. Isolation of CPM-RyR1 monomers is achieved using multiple large format SDS-PAGE, all yielding a similar fluorescent labeling pattern that is consistent with profiles generated in the initial detection of RyR1 hyperreactive sulfhydryls (30, 31), indicating successful labeling and repeatability of the SDS-PAGE separation. The lowest mobility fluorescence band from SDS-PAGE is excised, and the final peptide mass and sequence information confirm the excision of only RyR1.

SDS-PAGE also provides a good medium for full tryptic digestion of the CPM-RyR1, generating numerous peptides that are separated using sequential analytical and microbore HPLC. Tryptic digestion, a well documented method (36, 37), generates doubly charged cationic peptides, which generally fragment predictably in tandem mass spectrometric systems. Analytical HPLC separation generates a repeatable pattern of fluorescence peaks that are sequestered and concentrated into three groups, A, B, and C. The UV 214 absorbance profiles reveal numerous peaks, as expected from the 505 possible tryptic cleavage products of RyR1. The presence of a few, repeatable fluorescence peaks that do not overlap UV peaks attests to the specificity of CPM labeling and the selective, biologically relevant quantities of CPM used. The analytical HPLC groups A, B, and C contain several non-CPM-labeled RyR1 peptides, thus requiring an additional separation step achieved with microbore HPLC.

Fluorescence fractions from microbore HPLC are subjected to mass spectrometric analysis by two ionization methods (MALDI and ESI) to increase the chance of detection, because derivatized peptides often exhibit unpredictable and variable ionization behavior under different ionization techniques. Additionally, results supported by multiple MS methodologies increase the probability of successful identification.

The stringent criteria for mass comparisons between measured and theoretical masses (0.35 Da being the greatest difference in a peptide that was identified by MALDI and ESI), verification by multiple MS methodologies for five of seven cysteines, and the detection of the same CPM-adducted peptide in multiple HPLC fractions enables us to present the seven cysteines in Table I with very little uncertainty. For these seven cysteines, the probabilities presented may not correlate with the level of cysteine reactivity, because frequency and intensity of the MS signal may only be a function of gel extraction or ionization efficiency. However, the frequent position of the CPM-adducted cysteines near arginine or lysine residues may contribute to their hyperreactivity.

This possible of generation of cysteine hyperreactivity by juxtapositional arginines or lysines has potential implications for the lethal pharmacogenetic disorder malignant hyperther-

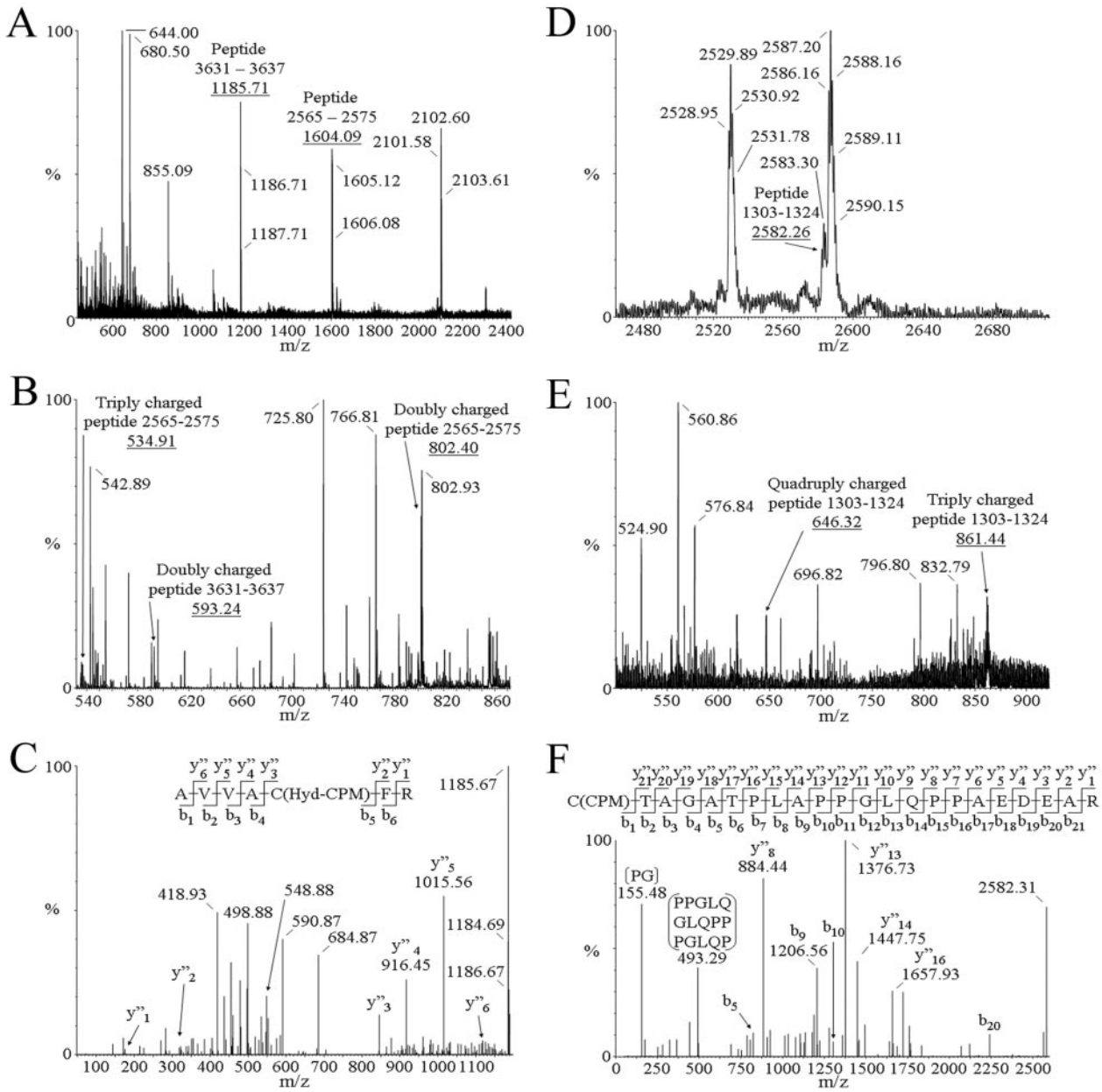

FIG. 4. **Mass spectrometry.** *A*, MALDI-TOF spectrum indicating monoisotopic masses that correspond to RyR1 peptide 3631–3637 with Cys-3635 adducted by hydrolyzed-CPM and peptide 2565–2575 with Cys-2565 adducted by CPM. *B*, direct ESI spectrum identifying doubly and triply charged ions corresponding to peptide 3631–3635 with Cys-3635 adducted by hydrolyzed-CPM and a doubly charged ion corresponding to peptide 2565–2575 with Cys-2565 adducted by CPM. *C*, an ESI MS/MS spectrum of the triply charged peptide from *part B*, which produces a fragmentation pattern that matches the predicted profile for peptide 3631–3637 with Cys-3635 adducted by hydrolyzed-CPM. *D*, MALDI-TOF spectrum indicating a monoisotopic mass that correspond to RyR1 peptide 1303–1324 with Cys-1303 adducted by hydrolyzed-CPM. *E*, direct ESI spectrum identifying triply and quadruply charged ions corresponding to peptide 1303–1324 with Cys-1303 adducted by hydrolyzed-CPM. *F*, an ESI MS/MS spectrum of the triply charged peptide from *part E*, which produces a fragmentation pattern that matches the predicted profile for peptide 1303–1324 with Cys-1303 adducted by hydrolyzed-CPM.

mia (MH) and the closely related central core disease (CCD), which are both linked to mutations in the *RyR1* gene. Human RyR1 R2435H/L mutations are associated with MH susceptibility (MHS) and CCD (38, 39), whereas R2454H/C (38, 40) and R2458H/C (41) mutations are associated with only MHS. Furthermore, a recent genetic and biochemical analysis of post-MH episode horse tissue reveals the point mutation R2454G (42). These arginine residues are vicinal to and possibly induce hyperreactivity in Cys-2436, the human analogue to rabbit Cys-2436 identified in this report. Non-arginine mutations vicinal to human Cys-2436 and linked to MHS include G2435H (40, 43, 44) and I2453T (45). Cys-2436 lies within a RyR1 MH/CCD region 2 (amino acids 2163–2458) that is often mutated in MHS or CCD patients; similarly, Cys-120, potentially identified here as a hyperreactive cysteine, lies within a RyR1 MH/CCD region 1 (amino acids 35–614) (46, 47). Although not necessarily related to MHS or CCD, the hyperreactivity, based on identification here, and the vicinal nature of cysteines of 2606 and 2611 suggest they may contribute the recently reported NADH-dependent oxidoreductase activity of RyR (48, 49).

This work presents the identification of hyperreactive sulfhydryls of RyR1 that may contribute to redox sensing and outlines a mass spectrometric methodology to identify reactive protein cysteines. Successful identification is derived from using a JSR preparation assayed for normal RyR1 function and

CPM labeling kinetics, employing a CPM-labeling procedure previously shown to selectively eliminate the RyR1 transmembrane redox sensor, SDS-PAGE fluorescence profiles matching the initial discovery of RyR1-hyperreactive sulfhydryls, repeatable analytical HPLC chromatograms with only six to eight fluorescence peaks, and the same CPM-adducted cysteines identified in multiple microbore HPLC fractions and via multiple MS methodologies. The possibility exists that the list of cysteines presented is not comprehensive, resulting from inefficient MS ionization or peptide extraction from the gel matrix. However, the seven hyperreactive cysteines identified in the present study provide a basis for focusing future molecular analysis using expression of Cys point mutations to unravel the redox-sensing mechanisms regulating the RyR1 complex. In addition, RyR1 mutations lacking inherent redox-sensing capabilities may help elucidate cell signaling cascades regulated by redox and better understand the physiological role of redox signaling.

Acknowledgments—We acknowledge the capable and timely support of Drs. Will Jewell and Young Moo Lee of the University of California, Davis Molecular Structure Facility with mass spectrometry.

REFERENCES

1. Floyd, R. A. (1990) *FASEB J.* **4,** 2587–2597
2. Floyd, R. A., and Carney, J. M. (1992) *Ann. Neurol.* **32,** (suppl.) S22–S27
3. Sigal, E., Laughton, C. W., and Mulkins, M. A. (1994) *Ann. N. Y. Acad. Sci.* **714,** 211–224
4. Butterfield, D. A., and Kanski, J. (2001) *Mech. Ageing Dev.* **122,** 945–962
5. Floyd, R. A. (1999) *Free Radic. Biol. Med.* **26,** 1346–1355
6. Gabbita, S. P., Robinson, K. A., Stewart, C. A., Floyd, R. A., and Hensley, K. (2000) *Arch. Biochem. Biophys.* **376,** 1–13
7. Pawloski, J. R., Hess, D. T., and Stamler, J. S. (2001) *Nature* **409,** 622–626
8. Stamler, J. S., Toone, E. J., Lipton, S. A., and Sucher, N. J. (1997) *Neuron* **18,** 691–696
9. Ignarro, L. J. (2002) *J. Cardiovasc. Surg.* **17,** 301–306
10. Koesling, D. (1999) *Methods* **19,** 485–493
11. Bolotina, V. M., Najibi, S., Palacino, J. J., Pagano, P. J., and Cohen, R. A. (1994) *Nature* **368,** 850–853
12. Manzoni, O., and Bockaert, J. (1993) *J. Neurochem.* **61,** 368–370
13. Sullivan, J. M., Traynelis, S. F., Chen, H. S., Escobar, W., Heinemann, S. F., and Lipton, S. A. (1994) *Neuron* **13,** 929–936
14. Eu, J. P., Sun, J., Xu, L., Stamler, J. S., and Meissner, G. (2000) *Cell* **102,** 499–509
15. Sun, J., Xin, C., Eu, J. P., Stamler, J. S., and Meissner, G. (2001) *Proc. Natl. Acad. Sci. U. S. A.* **98,** 11158–11162
16. Eager, K. R., Roden, L. D., and Dulhunty, A. F. (1997) *Am. J. Physiol.* **272,** C1908–C1918
17. Feng, W., Liu, G., Xia, R., Abramson, J. J., and Pessah, I. N. (1999) *Mol. Pharmacol.* **55,** 821–831
18. Salama, G., Abramson, J. J., and Pike, G. K. (1992) *J. Physiol.* **454,** 389–420
19. Trimm, J. L., Salama, G., and Abramson, J. J. (1986) *J. Biol. Chem.* **261,** 16092–16098
20. Bull, R., Marengo, J. J., Finkelstein, J. P., Behrens, M. I., and Alvarez, O. (2003) *Am. J. Physiol.* **285,** C119–C128
21. Feng, W., Liu, G., Allen, P. D., and Pessah, I. N. (2000) *J. Biol. Chem.* **275,** 35902–35907
22. Feng, W., and Pessah, I. N. (2002) *Methods Enzymol.* **353,** 240–253
23. Pessah, I. N., Kim, K. H., and Feng, W. (2002) *Front. Biosci.* **7,** a72–a79
24. Aracena, P., Sanchez, G., Donoso, P., Hamilton, S. L., and Hidalgo, C. (2003) *J. Biol. Chem.* **278,** 42927–42935
25. Donoso, P., Aracena, P., and Hidalgo, C. (2000) *Biophys. J.* **79,** 279–286
26. Marengo, J. J., Hidalgo, C., and Bull, R. (1998) *Biophys. J.* **74,** 1263–1277
27. Aghdasi, B., Zhang, J. Z., Wu, Y., Reid, M. B., and Hamilton, S. L. (1997) *J. Biol. Chem.* **272,** 3739–3748
28. Dulhunty, A., Haarmann, C., Green, D., and Hart, J. (2000) *Antioxid. Redox Signal.* **2,** 27–34
29. Sun, J., Xu, L., Eu, J. P., Stamler, J. S., and Meissner, G. (2001) *J. Biol. Chem.* **276,** 15625–15630
30. Liu, G., Abramson, J. J., Zable, A. C., and Pessah, I. N. (1994) *Mol. Pharmacol.* **45,** 189–200
31. Liu, G., and Pessah, I. N. (1994) *J. Biol. Chem.* **269,** 33028–33034
32. Oba, T., Murayama, T., and Ogawa, Y. (2002) *Am. J. Physiol.* **282,** C684–C692
33. Xia, R., Stangler, T., and Abramson, J. J. (2000) *J. Biol. Chem.* **275,** 36556–36561
34. Lowry, O. H., Rosenbrough, N. J., Farr, A. L., and Randall, R. J. (1951) *J. Biol. Chem.* **193,** 265–275
35. Saito, A., Seiler, S., Chu, A., and Fleischer, S. (1984) *J. Cell Biol.* **99,** 875–885
36. Shevchenko, A., Wilm, M., Vorm, O., and Mann, M. (1996) *Anal. Chem.* **68,** 850–858
37. Wilm, M., Shevchenko, A., Houthaeve, T., Breit, S., Schweigerer, L., Fotsis, T., and Mann, M. (1996) *Nature* **379,** 466–469
38. Barone, V., Massa, O., Intravaia, E., Bracco, A., Di Martino, A., Tegazzin, V., Cozzolino, S., and Sorrentino, V. (1999) *J. Med. Genet.* **36,** 115–118
39. Zhang, Y., Chen, H. S., Khanna, V. K., De Leon, S., Phillips, M. S., Schappert, K., Britt, B. A., Browell, A. K., and MacLennan, D. H. (1993) *Nat. Genet.* **5,** 46–50
40. Brandt, A., Schleithoff, L., Jurkat-Rott, K., Klingler, W., Baur, C., and Lehmann-Horn, F. (1999) *Hum. Mol. Genet.* **8,** 2055–2062
41. Manning, B. M., Quane, K. A., Lynch, P. J., Urwyler, A., Tegazzin, V., Krivosic-Horber, R., Censier, K., Comi, G., Adnet, P., Wolz, W., Lunardi, J., Muller, C. R., and McCarthy, T. V. (1998) *Hum. Mutat.* **11,** 45–50
42. Aleman, M., Riehl, J., Aldrich, B., LeCouteur, R., Stott, J., and Pessah, I. N. (2004) *Muscle Nerve*, in press
43. Keating, K. E., Quane, K. A., Manning, B. M., Lehane, M., Hartung, E., Censier, K., Urwyler, A., Klausnitzer, M., Muller, C. R., and Heffron, J. J. (1994) *Hum. Mol. Genet.* **3,** 1855–1858
44. Phillips, M. S., Khanna, V. K., De Leon, S., Frodis, W., Britt, B. A., and MacLennan, D. H. (1994) *Hum. Mol. Genet.* **3,** 2181–2186
45. Ruffert, H., Olthoff, D., Deutrich, C., and Froster, U. G. (2002) *Anaesthesist* **51,** 904–913
46. Jurkat-Rott, K., McCarthy, T., and Lehmann-Horn, F. (2000) *Muscle Nerve* **23,** 4–17
47. McCarthy, T. V., Quane, K. A., and Lynch, P. J. (2000) *Hum. Mutat.* **15,** 410–417
48. Baker, M. L., Serysheva, I. I., Sencer, S., Wu, Y., Ludtke, S. J., Jiang, W., Hamilton, S. L., and Chiu, W. (2002) *Proc. Natl. Acad. Sci. U. S. A.* **99,** 12155–12160
49. Xia, R., Webb, J. A., Gnall, L. L., Cutler, K., and Abramson, J. J. (2003) *Am. J. Physiol.* **285,** C215–C221